DALTON

Soft cobalt(III) centres: electronic levelling in $[CoX_3(AH_3)_2]$ (X = Cl, Br or I; A = P, As or Sb)*

Robert J. Deeth

Inorganic Computational Chemistry Group, Department of Chemistry, University of Warwick, Coventry, UK CV4 7AL

The geometric and electronic structures of the trigonal-bipyramidal cobalt(III) complexes of general formula $[CoX_3(AH_3)_2]$ (X = Cl, Br or I; A = P, As or Sb) have been computed using density functional theory (DFT). The performance of the local density approximation (LDA) and three different gradient-corrected functionals has been evaluated by comparing the computed structure of $[CoI_3(PH_3)_2]$ with that observed for the PPh_3 analogue. This molecule, plus $[CoI_3(AsH_3)_2]$ and $[CoCl_3(SbH_3)_2]$, the last two being compared with the observed PMe_3 systems, were used to test the performance of different basis sets. The LDA gives too short bond lengths. However, computed structures using gradient-corrected DFT are in good agreement with experiment. The Co–P and Co–Sb bond lengths are systematically underestimated but full calculations for the trimethyl derivatives indicate this is due to the use of a model AH_3 moiety. The calculations show all the complexes to be paramagnetic spin triplets and reveal a remarkable electronic levelling such that the frontier molecular orbital energies are virtually independent of X or A. Estimates of the Co–A bond energies are also very similar for all nine molecules spanning the narrow range 191–217 kJ mol^{-1}. These data indicate comparable stabilities across the entire series. The unique features of these molecules result in a 'soft' metal centre despite its formal +3 charge. The balance between five- and six-co-ordination is discussed using calculations on the *fac* and *mer* isomers of the hypothetical $[CoI_3(PH_3)_3]$ complex.

The dihalogen adducts of phosphines, arsines and stibines show remarkable activity towards transition metals.[1–7] They are capable of oxidising unactivated metal powders to produce a range of di- and tri-valent metal species. A particularly interesting and fairly general reaction results in the formation of unusual trigonal-bipyramidal complexes of general formula $[MX_3(AR_3)_2]$, where X is a halogen and A is a Group 15 element.

With cobalt metal powder the resulting complexes are rare examples of paramagnetic cobalt(III) species. This is a direct consequence of the trigonal-bipyramidal ligand field where the orbital sequence d_{xz}, $d_{yz} < d_{x^2-y^2}$, $d_{xy} < d_{z^2}$ and the d^6 configuration must lead to unpaired electrons. The unusual feature is not the paramagnetism but rather the five-co-ordination. The cobalt(III) oxidation state is normally associated with low-spin six-co-ordinate complexes for which the ligand-field stabilisation energy is a maximum. Stranger still is the observation of Co–P,[5] Co–As [1] and Co–Sb bonds.[2] Cobalt(III) is normally considered a hard metal centre which favours co-ordination to second-row atoms like oxygen and nitrogen. These $[CoX_3(AR_3)_2]$ species do not conform to normal expectations.

In order to probe the factors which determine the stabilities of these compounds, a series of *ab initio* density functional theory (DFT) calculations was undertaken. DFT is proving to be an extremely valuable tool for modelling the structures and reactivities of transition-metal systems.[8,9] One issue which has been explored recently concerns the relative performance of local *versus* gradient corrected functionals for calculating the structures and binding energies of Werner-type and organometallic complexes.[10,11] The metal–ligand bond lengths of Werner species seem to be better reproduced with local density approximation (LDA) calculations while organometallic species, such as metal carbonyls, require gradient-corrected DFT. Cobalt(III) would normally be considered to form Werner species but the chemistry of these $[MX_3(AR_3)_2]$ species seems rather more akin to organometallic compounds. Accordingly, it is of interest computationally to investigate the relative performance of local and gradient corrected schemes to see whether this continues to provide a phenomenological distinction between Werner-type and organometallic chemistry.

* *Non-SI unit employed*: eV ≈ 1.60×10^{-19} J.

Computational Details

All calculations were performed with the Amsterdam Density Functional (ADF) program version 2.0.1 or 2.3.0.[12–14] The implementation of the local density approximation uses the standard Slater exchange term [15] and the correlation term due to Vosko *et al.*[16] Geometries were optimised using analytical energy gradients [17,18] usually within a spin-restricted formalism. Other studies have demonstrated that for systems up to $S = 1$, spin-restricted and -unrestricted DFT geometries are the same.[19,20] Three gradient-corrected functionals were also considered: BP refers to the combination of Becke's 1988 exchange correction [21] and Perdew's 1986 correlation functional,[22] PW91 to the functional proposed by Perdew and Wang in 1991 [23] while BLYP refers to Becke's 1988 exchange functional plus the correlation functional due to Lee *et al.*[24] The BLYP calculations are the only ones where ADF version 2.3.0 was employed.

Basis sets comprised uncontracted triple-ζ expansions of Slater-type orbitals (ADF basis sets IV). All bases were augmented by additional functions (p on metals and H, d on the rest). Polarisation function for iodine and Sb are not in the standard ADF release so 5d orbitals with exponent 1.8 were added. The frozen-core approximation [25] was used throughout: 1s on carbon; 1s–2p on Co, P and Cl; 1s–3p or 1s–3d on As and Br; 1s–4p or 1s–4d on Sb and I. The frozen-core nomenclature is of the form El:[*nl*] where El is the relevant element symbol, *n* the principal quantum number, *l* the angular momentum quantum number, and all orbitals 1s through *nl* are frozen. The effect of the frozen-core size was investigated as described below.

The geometries of all the five-co-ordinate complexes were constrained to D_{3h} symmetry resulting in four independent variables for AH_3 complexes and eight independent variables for AMe_3 complexes. The Co–A bond strength was estimated as half the binding energy between CoX_3 and two AH_3 fragments.

Table 1 Calculated and observed (in italics) bond lengths (Å) and angles (°) for $[CoX_3(AH_3)_2]$ systems for various functionals and atomic frozen cores

X:A	Functional	X core	A core	Co–X	Co–A	A–H	Co–A–H
I:P	LDA	4p	2p	2.48	2.16	1.43	118
I:P	LDA	4d	2p	2.51	2.16	1.43	118
I:P	BP	4p	2p	2.57	2.22	1.43	118
I:P	BP	4d	2p	2.62	2.22	1.43	118
I:P	BLYP	4p	2p	2.60	2.21	1.41	118
I:P	PW91	4p	2p	2.57	2.20	1.43	118
	(*R* = *Me*)[a]			*2.55*	*2.28*		
I:As	BP	4p	3p	2.57	2.33	1.52	118
I:As	BP	4p	3d	2.57	2.34	1.54	118
	(*R* = *Me*)[b]			*2.52*	*2.33*		
I:Sb	BP	4p	4p	2.59	2.49	1.72	119
I:Sb	BP	4p	4d	2.60	2.50	1.75	119
	(*R* = *Ph*)[c]			*2.57*	*2.59*		
Br:P	BP	3p	2p	2.37	2.22	1.43	118
Br:As	BP	3p	3p	2.38	2.33	1.52	118
Br:I	BP	3p	4p	2.38	2.51	1.72	119
Cl:P	BP	2p	2p	2.23	2.23	1.43	117
	(*R* = *Et*)[d]			*2.20*	*2.28*		
Cl:As	BP	2p	3p	2.22	2.33	1.52	118
Cl:I	BP	2p	4p	2.23	2.51	1.72	119

[a] Ref. 5. [b] Ref. 1. [c] Ref. 2. [d] Ref. 28.

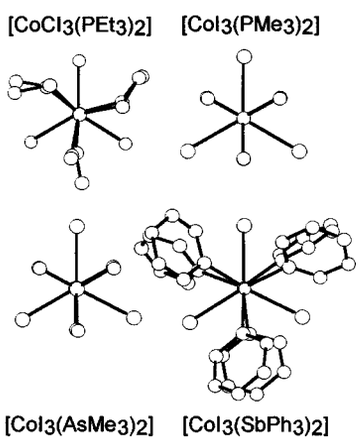

Fig. 1 Views of the molecular structures derived from X-ray diffraction studies of several $[CoX_3(AR_3)_2]$ species (H atoms omitted)

This was calculated using Ziegler and Rauk's extended transition state (ETS) method[26,27] with the energies of the separate fragments computed at their 'in-molecule' configurations; D_{3h} symmetry was used for CoX_3 and C_{3v} for AH_3. The symmetries for *fac* and *mer* isomers of the hypothetical $[CoI_3(PH_3)_3]$ complex were C_{3v} and C_s respectively.

Default convergence criteria were used apart from the numerical integration factor which was set to 4 (the default value is 3).

Results and Discussion

Molecular structures

Single-crystal X-ray diffraction studies have been reported for $[CoI_3(PMe_3)_2]$,[5] $[CoCl_3(PEt_3)_2]$,[28] $[CoI_3(AsMe_3)_2]$[1] and $[CoI_3(SbPh_3)_2]$.[2] Fig. 1 shows these structures viewed down the notional three-fold axis. To a good approximation, the substituents on the axial donors are mutually eclipsed with respect to each other and staggered with respect to the equatorial halides. The highest possible symmetry is therefore D_{3h} and this point group was imposed on all geometry optimisations.

The observed Co–L distances are the basis for determining the optimum combination of functional and basis set. Experience has shown that triple-ζ + polarisation bases (ADF set IV) are sufficiently flexible. However, the computed results do depend on the size of the frozen core. For first-row transition metals the 3s and 3p orbitals are always explicitly included in the valence set (*i.e.* an M:[2p] frozen core). For the elements beyond argon there are two choices for the size of the frozen core depending on whether a set of d orbitals is included in the valence set or not. The normal expectation is that the calculations should give rise to metal–ligand bond lengths within about ±0.02–0.04 Å of experiment.[9]

The results of geometry optimisations for all nine $[CoX_3(AH_3)_2]$ species are collected in Table 1 along with any available experimental data. A thorough set of calculations was undertaken for $[CoI_3(PH_3)_2]$. The LDA results appear to underestimate the Co–L distances, particularly Co–P, although part of this is due to using PH_3 instead of the actual phosphine PMe_3 (see below). The best results are obtained with the smaller I:[4p] frozen core on I and with one of the gradient-corrected functionals. Becke 88–Perdew 86 (BP) is marginally better than Perdew–Wang 91 (PW91) or Becke 88–Lee–Yang–Parr (BLYP) and gives a Co–I distance 0.02 Å longer than experiment and a Co–P distance 0.06 Å shorter. The BP functional and I:[4p] basis was used subsequently. For $[CoI_3(AsH_3)_2]$ and $[CoI_3(SbH_3)_2]$ the size of the frozen core has little effect on the Co–As or Co–Sb distances. Where applicable, the smaller frozen core is employed for the remaining calculations.

To summarise, using the BP gradient-corrected functional, small frozen-core bases and AH_3 model ligands, the Co–X bonds are systematically overestimated by between 0.02 to 0.05 Å, while the Co–A distances are calculated too short by up to twice this range. However, the latter can be traced to the use of AH_3 model ligands. Calculations on the complete $[CoI_3(AMe_3)_2]$ systems (A = P or As) lengthen the Co–P bond by 0.08 Å and the Co–As bond by 0.04 Å (Table 2). All the Co–L distances are now systematically slightly too long. The maximum discrepancy is the Co–I distance in $[CoI_3(AsMe_3)_2]$ which is some 0.06 Å longer than experiment.

Overall, the AH_3 ligands reproduce the observed structures fairly well with errors which are reasonably systematic. Therefore, for simplicity and to maintain consistency, AH_3 ligands are employed in the rest of this paper.

Table 2 Calculated and observed (in italics) bond lengths (Å) for $[CoX_3(AMe_3)_2]$ systems for the Becke 88–Perdew 86 gradient-corrected functional and small frozen cores (see text)

X:A	Functional	Co–X	Co–A
I:P	BP	2.59	2.30
		2.55	*2.28*
I:As	BP	2.58	2.37
		2.52	*2.33*

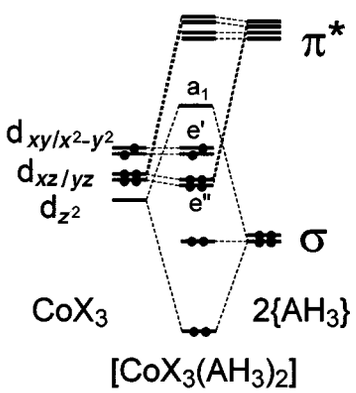

Fig. 2 Qualitative partial molecular orbital energy-level diagram for $[CoX_3(AH_3)_2]$ complexes. Note the d-orbital labels do not refer to free Co^{III} but to the valence orbitals of CoX_3 with predominantly d-orbital character

Gradient-corrected DFT gives satisfactory geometries for these complexes which contrasts with its performance for more classical species where the LDA already tends to give too long M–L distances and the gradient corrections make the comparison with experiment worse.[10] Qualitatively, there is a correlation between covalency and DFT bond distances with more ionic systems (*i.e.* Werner-type complexes) treated better by the LDA. The present molecules are very covalent (see below) and give charge distributions well removed from those suggested by formal oxidation states. This near electroneutrality is more typical of organometallic compounds which correlates with these $[CoX_3(AH_3)_2]$ species being treated better by gradient-corrected DFT.

Electronic structures and charge distributions

A qualitative molecular orbital energy-level scheme for these $[CoX_3(AH_3)_2]$ systems is shown in Fig. 2. Only the interactions between the AH_3 frontier orbitals and the valence, mainly d functions on the CoX_3 fragment are depicted. Note that the lowest spin-triplet state for the latter is non-*aufbau* with the empty a_1' (mainly d_{z^2}) function lying below the fully occupied e″ (mainly d_{xz}, d_{yz}) and the half-filled e′ (mainly d_{xy}, $d_{x^2-y^2}$) orbitals. The main interaction is the σ binding between the empty a_1' ($\approx d_{z^2}$) on the metal centre of CoX_3 and the filled in-phase combination of lone-pair functions on the AH_3 ligands. As detailed below, π bonding is less important since the π* functions of the AH_3 moieties are both too high in energy and possess significant A–H σ character.

Despite the variation in both X and A, the valence orbital structures of all nine complexes are remarkably similar. This is shown graphically in Fig. 3. Strong electronic levelling is evident especially for the highest occupied e′ functions which shift by only a few tenths of an eV compared to a drop in the first ionisation potentials of around 2.5 eV for iodine compared to chlorine and 1.9 eV for antimony compared to phosphorus. There is a periodic trend in the energy of the e″ orbital, but again the actual shifts are relatively small. The energies of the a_1' orbitals decrease as a function of X but do not vary monotonically as a function of AH_3. The latter change can be traced to the MO compositions (Figs. 4–6). The main contribution to

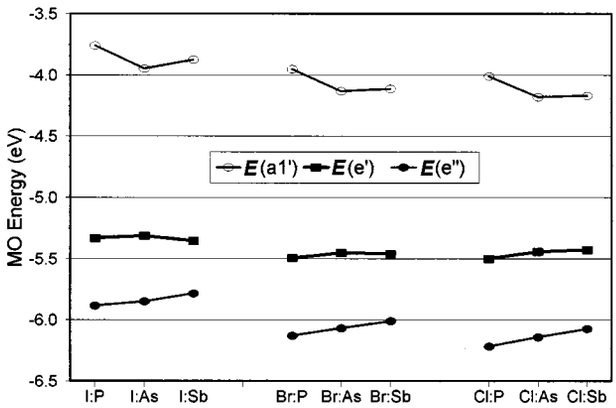

Fig. 3 Valence molecular orbital energies (eV) for $[CoX_3(AH_3)_2]$ species. The e″ functions are filled, the e′ functions half-filled and the a_1' functions are empty

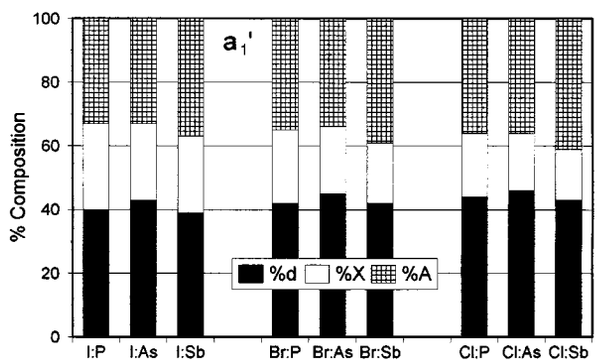

Fig. 4 Percentage compositions of valence a_1' molecular orbitals (see Fig. 3 for the energy)

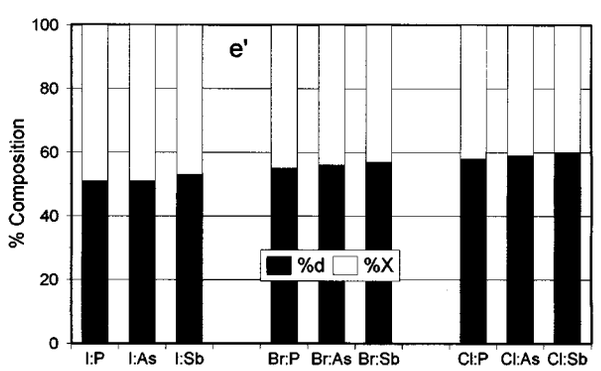

Fig. 5 Percentage compositions of valence e′ molecular orbitals (see Fig. 3 for the energy)

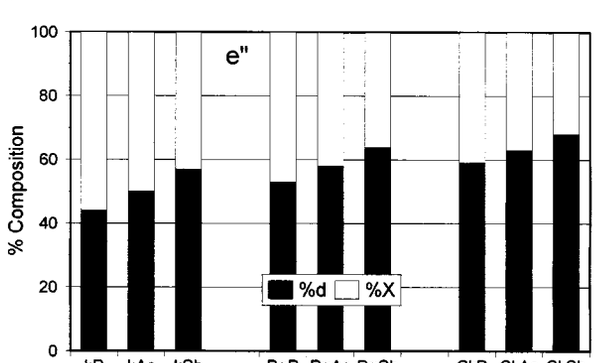

Fig. 6 Percentage compositions of valence e″ molecular orbitals (see Fig. 3 for the energy)

a_1' from P and As (Fig. 4) arises from their p orbitals. At Sb the valence 5s orbital is now sufficiently high in energy to make a contribution. The overall cobalt contribution remains fairly steady at about 40–45%.

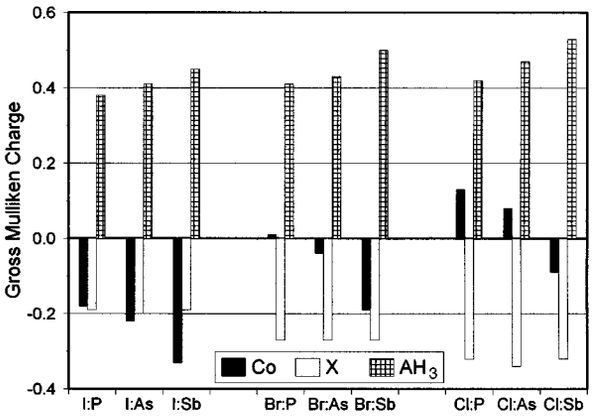

Fig. 7 Gross Mulliken charges on cobalt, X and AH_3 fragments

Table 3 Calculated Co–A bond energies *E*(Co–A) and its breakdown into steric and orbital overlap components. The last column gives the amount of the orbital interaction concentrated in the σ-bonding a_1' interaction. All data in kJ mol^{-1}

X:A	*E*(Co–A)	*E*(steric)	*E*(orb)	*E*(orb):a_1'
I:P	−217	166	−600	−375
I:As	−193	155	−541	−353
I:Sb	−191	165	−547	−392
Br:P	−217	154	−588	−382
Br:As	−196	137	−528	−360
Br:Sb	−191	168	−550	−391
Cl:P	−220	138	−579	−395
Cl:As	−195	138	−528	−377
Cl:Sb	−191	164	−546	−381

The composition of the e′ orbitals also describes a very covalent picture with cobalt d contributions of around 50% for X = I rising to around 60% for X = Cl (Fig. 5). The AH_3 moieties do not contribute since the Co–A interaction is formally of δ symmetry and the overlap is too small. The e″ orbitals are also strong mixtures of cobalt d and X p orbitals (Fig. 6). Despite the e″ functions being formally of the correct symmetry for Co–A π interactions, the latter do not appear. The π-acceptor orbitals on these AH_3 model ligands are essentially A–H σ functions. If only valence p orbitals are considered on A the interaction is σ antibonding and the orbital is at high energy, but when d orbitals on A are included there is a much lower energy function where the interaction is A–H σ bonding. There is about a 20% d orbital component which could mediate the Co–AH_3 π* interaction but is apparently either too small or too involved with the A–H bonding (or both) to make a significant contribution. This also applies to PMe_3 ligands where their total contribution to the filled valence e″ orbital of $[CoI_3(PMe_3)_2]$ is less than 2%. Evidently, the AR_3 ligands do not depend on any π character for forming strong Co–A bonds.

Another clue to the unusual behaviour of these complexes comes from the computed charge distributions. These are based on Mulliken population analyses and should only be considered to give a qualitative guide. The charges on Co, X and the AH_3 ligands are shown in Fig. 7. The most striking feature is that the charge on X remains essentially constant as A changes from P to As to Sb. In contrast, the AH_3 groups become increasingly positive in the order $PH_3 < AsH_3 < SbH_3$. This increase in ligand-to-metal charge donation is mirrored by a correspondingly more negative charge on Co. These observations are consistent with σ-dominated Co–A bonding which, being mediated through the metal d_{z^2} orbital which is itself concentrated along the A–Co–A direction, effectively decouples the halides from the $\{H_3A–Co–AH_3\}$ unit.

The charge on X is about −0.2 for X = I, −0.28 for X = Br and −0.33 for X = Cl, which is consistent with the more electronegative the halide, the higher its negative charge, and this correlates with a generally more positive cobalt centre. Nevertheless, relative to the formal charge on X of −1, all the halide ligands are donating strongly to the metal making it much more electron rich than its formal charge of +3 would suggest.

The principal effect of the X to Co charge donation is to raise the frontier-orbital energies of the CoX_3 fragment so that they can interact effectively with the AR_3 ligands. This applies particularly to the a_1' function which is involved in the important Co–A σ interactions. The symmetry also facilitates the fairly clean separation between Co–X and Co–A σ bonding since only d_{x^2} connects axial and equatorial groups and this orbital is dominated by axial interactions.

Co–A bond strengths

The above analysis points to halide ligands which seem to be effectively decoupled from the Co–A interactions. This is further reflected in the estimates of the Co–A binding energies (Table 3). The Co–P, Co–As and Co–Sb binding energies are around −220, −195 and −191 kJ mol^{-1} respectively. These values vary by less than 3 kJ mol^{-1} as a function of X. Note that the overall variation of binding energies is far smaller than the orbital energy changes depicted in Fig. 3. This is because the functions shown are not the only ones contributing to the M–L binding. All nine species are predicted to have similar stabilities and indeed complexes representing the extrema of the examples considered here, *i.e.* $[CoCl_3(PMe_3)_2]$ and $[CoI_3(SbPh_3)_2]$, have been isolated and structurally characterised.

The total binding interaction can be divided into a steric and an orbital component, *E*(steric) and *E*(orb) respectively. The steric component represents the energy cost of bringing the interacting fragments up to their bonding positions but without allowing their charge clouds to overlap; *E*(orb) then represents the energy gain from the subsequent orbital overlap. For net binding, *E*(orb) must be greater in magnitude than *E*(steric) and have the opposite sign. The dominant contribution to *E*(orb) comes from the σ interaction of a_1' symmetry amounting to some 60–70% (last column, Table 3); *E*(steric) becomes smaller in the sequence I > Br > Cl but *E*(orb) also becomes less negative such that the sum of *E*(orb) and *E*(steric) is independent of X. The Co–P bonds are the strongest which seems mainly due to a favourable *E*(orb). The Co–As and Co–Sb bonds have comparable strengths.

Five- *versus* six-co-ordination

One of the intriguing aspects of these complexes is what makes the five-co-ordinate, trigonal-bipyramidal geometry so special compared to the more commonly observed six-co-ordinate cobalt(III) species. An estimate of the tendency for $[CoI_3(PH_3)_2]$ to attach a third phosphine molecule can be computed from the total binding energies. The 'product' $[CoI_3(PH_3)_3]$ could exist in *fac* or *mer* isomeric forms. Optimised geometries and selected geometrical parameters are shown in Fig. 8.

The Co–P distances remain unchanged relative to $[CoI_3(PH_3)_2]$ but the Co–I bonds are now some 0.1 Å longer. The *mer* isomer is about 60 kJ mol^{-1} more stable than the *fac* isomer. The latter is 1 kJ mol^{-1} *less* stable than $[CoI_3(PH_3)_2] + PH_3$. Hence, the energy gain from adding an additional phosphine to form the *mer* isomer is about 60 kJ mol^{-1}. {Note that here the energy of $[CoI_3(PH_3)_2]$ was recalculated within a spin unrestricted formalism which lowered the energy relative to the spin-restricted value by some 60 kJ mol^{-1}.} Given that the Co–P bonds in $[CoI_3(PH_3)_2]$ have an energy of about 220 kJ mol^{-1}, the *mer* isomer is predicted to have a relatively low stability and this picture may even be reversed if bulkier phosphines are employed.

The longer, presumably weaker, Co–I bonds in $[CoI_3(PH_3)_3]$

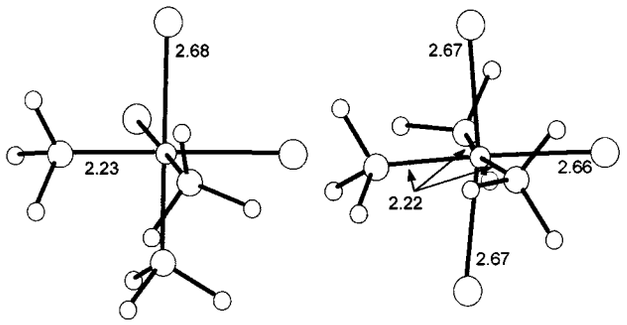

Fig. 8 Calculated structures and Co–L bond lengths (Å) for $[CoI_3(PH_3)_3]$

are consistent with both the extra steric demands of six-co-ordination and the effect of increased ligand-to-metal charge donation. The latter would tend to make the metal even more electron rich and thus less willing to accept charge from the ligands. This appears to affect only the halides. Apparently, five-co-ordination represents a more favourable balance between steric and electronic factors and will also benefit from an increased entropy relative to a six-co-ordinate species.

Conclusion

The geometric structures of nine trigonal-bipyramidal $[CoX_3(AH_3)_2]$ complexes were calculated using DFT. The optimum combination of basis sets and gradient-corrected functional was chosen based on a comparison of calculated and experimental bond lengths. The Becke 88–Perdew 86 functional, in combination with triple-ζ + polarisation basis sets and small frozen cores, yields acceptable results. Full optimisations of $[CoI_3(PMe_3)_2]$ and $[CoI_3(AsMe_3)_2]$ show that the systematic underestimate of the Co–A distances is due to the use of AH_3 model ligands.

The electronic structures show a remarkable levelling effect such that the energy of the highest occupied molecular orbital is essentially independent of X and A. The electron distributions further showed that the charges on X are independent of A and that any change in the donation from A is accommodated by the metal. However, the calculated Co–A bond energies stay fairly constant spanning the range 220 to 191 kJ mol^{-1}. All nine species are predicted to have comparable stabilities. The metal centre is much more electron rich than its formal oxidation state suggests. The special features of the CoX_3 fragment ensure that there is a relatively high-lying empty a_1' orbital available to form strong σ interactions with any donor approaching along the *z* axis with Co–A π interactions being virtually non-existent even though the AH_3 π* orbitals have a significant d-orbital component (≈20%) of the correct symmetry to interact with the Co d_{xz} and d_{yz} functions. This leads to an effective decoupling of the halides from the $\{H_3A–Co–AH_3\}$ unit.

The factors favouring five- *versus* six-co-ordination in these formally cobalt(III) complexes were explored *via* calculations on the hypothetical *fac* and *mer* isomers of $[CoI_3(PH_3)_3]$. The former has a slightly higher energy than $[CoI_3(PH_3)_2] + PH_3$ while the latter is only about 60 kJ mol^{-1} more stable. With bulkier phosphines the extra crowding around a six-co-ordinate centre might result in the *mer* isomer having a higher energy than its isolated components also. The higher steric and electronic demands of six-co-ordination result in longer, presumably weaker, Co–I bonds which is consistent with the tendency for these complexes to form less crowded five-co-ordinate species. The latter with a free ligand is also favoured by entropy.

Despite the formally 'hard' cobalt(III) centre, these systems behave chemically and theoretically as organometallic species. Computationally, this is manifest in gradient-corrected DFT giving a better description of the structures and binding energies than does the LDA.

Acknowledgements

The author acknowledges the support of the Engineering and Physical Sciences Research Council and the University of Warwick for provision of computer hardware and Professor C. A. McAuliffe for suggesting the problem.

References

1 N. Bricklebank, S. M. Godfrey, C. A. McAuliffe and R. G. Pritchard, *J. Chem. Soc., Dalton Trans.*, 1996, 157.
2 S. M. Godfrey, C. A. McAuliffe and R. G. Pritchard, *J. Chem. Soc., Chem. Commun.*, 1994, 45.
3 S. M. Godfrey, C. A. McAuliffe and R. G. Pritchard, *J. Chem. Soc., Dalton Trans.*, 1993, 2875.
4 S. M. Godfrey, H. P. Lane, C. A. McAuliffe and R. G. Pritchard, *J. Chem. Soc., Dalton Trans.*, 1993, 1599.
5 C. A. McAuliffe, S. M. Godfrey, A. G. Mackie and R. G. Pritchard, *Angew. Chem., Int. Ed. Engl.*, 1992, **31**, 919.
6 S. M. Godfrey, D. G. Kelly, A. G. Mackie, P. P. M. Rory, C. A. McAuliffe, R. G. Pritchard and S. M. Watson, *J. Chem. Soc., Chem. Commun.*, 1991, 1447.
7 B. Beagley, C. A. McAuliffe, K. Minten and R. G. Pritchard, *J. Chem. Soc., Dalton Trans.*, 1987, 1999.
8 M. R. Bray, R. J. Deeth and V. J. Paget, *Prog. React. Kinet.*, 1996, **21**, 169.
9 R. J. Deeth, *Struct. Bonding* (*Berlin*), 1995, **82**, 1.
10 M. R. Bray, R. J. Deeth, V. J. Paget and P. D. Sheen, *Int. J. Quantum Chem.*, 1997, **61**, 85.
11 R. J. Deeth and H. D. B. Jenkins, *J. Phys. Chem.*, 1997, **101**, 4793.
12 ADF version 2, Theoretical Chemistry, Vrije Universiteit, Amsterdam, 1993–1997.
13 E. J. Baerends, D. E. Ellis and P. Ros, *Chem. Phys.*, 1973, **2**, 41.
14 G. te Velde and E. J. Baerends, *J. Comput. Phys.*, 1992, **99**, 84.
15 J. C. Slater, *Adv. Quantum Chem.*, 1972, **6**, 1.
16 S. H. Vosko, L. Wilk and M. Nusair, *Can. J. Phys.*, 1980, **58**, 1200.
17 L. Y. Fan and T. Ziegler, *J. Chem. Phys.*, 1991, **95**, 7401.
18 L. Versluis and T. Ziegler, *J. Chem. Phys.*, 1988, **88**, 322.
19 R. J. Deeth, *J. Chem. Soc., Dalton Trans.*, 1995, 1537.
20 P. D. Sheen, Ph.D. Thesis, University of Bath, 1995.
21 A. D. Becke, *Phys. Rev. A*, 1988, **38**, 3098.
22 J. P. Perdew, *Phys. Rev. B*, *Condensed Matter*, 1986, **33**, 8822.
23 J. P. Perdew, *Physica B*, 1991, **172**, 1.
24 C. T. Lee, W. T. Yang and R. G. Parr, *Phys. Rev. B*, *Condensed Matter*, 1988, **37**, 785.
25 E. J. Baerends, D. E. Ellis and P. Ros, *Theor. Chim. Acta*, 1972, **27**, 339.
26 T. Ziegler and A. Rauk, *Inorg. Chem.*, 1979, **18**, 1558.
27 T. Ziegler and A. Rauk, *Inorg. Chem.*, 1979, **18**, 1755.
28 W. J. P. van Enckevort, H. M. Hendricks and P. T. Beurskens, *Cryst. Struct. Commun.*, 1977, **6**, 531.

Received 24*th July* 1997; *Paper* 7/05370C